NBSIR 74-485

Strength of Glass--A Fracture Mechanics Approach

S. M. Wiederhorn

Inorganic Materials Division
Institute for Materials Research
National Bureau of Standards
Washington, D.C. 20234

May 1974

Interim Report for Period July 1, 1973 through June 30, 1974

Prepared for

Department of the Navy
Office of Naval Research
Arlington, Virginia 22217

NBSIR 74-485

STRENGTH OF GLASS--A FRACTURE MECHANICS APPROACH

S. M. Wiederhorn

Inorganic Materials Division
Institute for Materials Research
National Bureau of Standards
Washington, D.C. 20234

May 1974

Interim Report for Period July 1, 1973 through June 30, 1974

To be published in Proceedings of Tenth International Congress on Glass, Kyoto, Japan, July 8-13, 1974

Prepared for
Department of the Navy
Office of Naval Research
Arlington, Virginia 22217

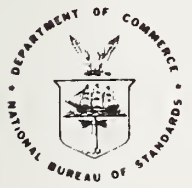

U. S. DEPARTMENT OF COMMERCE, Frederick B. Dent, Secretary
NATIONAL BUREAU OF STANDARDS, Richard W. Roberts, Director

ABSTRACT

After a brief review of those factors that determine the strength of glass (brittleness, surface flaws, susceptibility to stress corrosion cracking), a discussion will be given of how fracture mechanics techniques can be used to understand the physics and chemistry of glass strength. In this paper we assume that the strength of glass is limited by the growth of cracks that are always present in normal glass surfaces. Fracture mechanics techniques can be used to characterize the crack growth and to relate the growth to experimental parameters such as temperature, environment and glass composition. Crack growth data obtained in this manner can be used to develop a deeper understanding of fracture mechanisms, and to develop charts that can be used for the design of glass structural components. Examples of both applications are given in this paper.

INTRODUCTION

In this paper fracture mechanics is discussed: as a method of understanding the strength of glass, and as a method of providing data that can be used to assure the structural reliability of glass. A review is first presented of the main factors that control the strength of glass (temperature, environment, surface condition, etc.). Then fracture mechanics techniques are described, and the available fracture mechanics data are reviewed. Finally, the use of fracture mechanics for failure prediction is discussed.

REVIEW OF THE LITERATURE ON THE STRENGTH OF GLASS

The two main characteristics that determine the strength of glass are brittle behavior and static fatigue. Glass is one of the most brittle materials known because at low temperatures deformation is almost completely elastic. This elasticity has been demonstrated on silica rods and fibers by Hillig (Ref. 1) and by Mallinder and Proctor (Ref. 2) to loads as high 1.1 GN/m^2 (1.6×10^6 psi), and on soda lime silicate glass fibers by Mallinder and Proctor (Ref. 2) to 0.4 GN/m^2 (0.6×10^6 psi). The stresses were so high in these experiments that non-linear elastic behavior was observed; however, the deformation completely disappeared when the load was released. Interestingly, the Youngs modulus for the silica glass increased during these experiments, while that for soda lime silicate glass decreased.

Permanent deformation can occur in glass under certain circumstances. Permanent densification has been observed by Bridgeman (Ref. 3) and by Cohen and Roy (Ref. 4) on glasses that have been subjected to pressures of 7 GN/m^2 (10^6 psi). During hardness indentation tests, plastic flow and densification occurs because of the high compressive and shear stresses ($\sim$ 10 GN/m^2) near the indenter (Ref. 5,6). Permanent deformation has also been observed in compressive tests conducted by Ernsberger (Ref. 7) on glass rods that contained oblate bubbles. In these experiments densification was observed in Pyrex and silica glass at stresses of approximately 7 GN/m^2. In all of the above cases, high compressive loads were necessary for the occurrence of plastic deformation. To date, there have been no unequivocal reports of plastic deformation of glass that has been subjected to tensile loads.

The low strength of glass is a direct result of this brittle behavior. When glass is polished and ground, small cracks are left in the glass surface.[8] These cracks act as stress concentrators so that the crack tip stress is considerably higher than the average applied stress. Since plastic deformation does not occur to relieve these crack tip stresses, the surface cracks propagate when a critical stress is reached at the crack tip. The critical stress required for crack motion is determined in part by the glass composition, and in part by the environment at the crack tip. The environmental contribution to crack motion results in a time dependence of strength known as static fatigue.

Static fatigue of glass was observed first by Grenet (Ref. 9) who noted a time dependence of strength for both static and dynamic loading conditions. For a constant loading rate, the strength depended on the rate of loading, increasing as the rate increased; whereas for constant load, failure occurred after a period of time at load. The phenomenon of static fatigue at constant load is illustrated in figure 1.

The failure time depends on the load applied to the glass; large loads can only be supported for short periods of time. If the load is small enough, a fatigue limit occurs; fracture does not occur regardless of the time for which the load is applied.

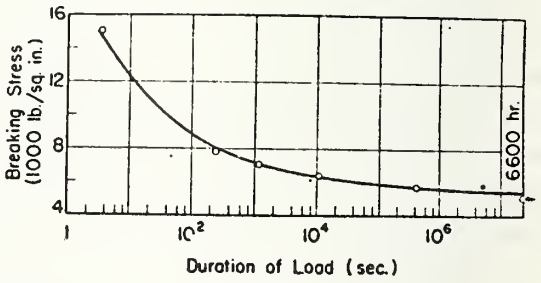

Fig. 1 Static fatigue of soda-lime silicate glass (Ref. 10)

Static fatigue can be explained by the growth of cracks caused by a stress enhanced chemical reaction between water and glass. Static fatigue occurs only in the presence of water which reacts chemically with the strained bonds at the crack tip causing bond rupture. The rate of crack growth is determined by the rate of the chemical reaction, and the time to failure is determined by the time required for the crack to grow from a subcritical to a critical size, at which point, failure is instantaneous.

Before the advent of fracture mechanics concepts, strength measurements were used to study static fatigue. The strength was measured in three or four point loading as a function of loading rate, or the time to failure was measured as a function of applied load. Using these techniques the following observations were made:

o Static fatigue occurred only in the presence of water (Ref. 11-14).

o Static fatigue could be detected for load times as short as 10^{-2} second (Ref. 14).

o Static fatigue did not occur in a vacuum or at very low temperatures (-196°C) (Ref. 12, 13, 15).

o Static fatigue was an activated process, fracture becoming easier at higher temperatures (Ref. 16, 17).

o Static fatigue was the result of a single process that did not depend on the surface flaw size (Ref. 18).

o The static fatigue limit occurs at approximately 20-30 percent of the environment-free strength (Ref. 10, 19).

While strength studies provided considerable information on the strength of glass and the occurrence of static fatigue, fracture mechanics techniques added to this body of knowledge, providing a deeper insight into the fracture process.

FRACTURE MECHANICS TECHNIQUES

Fracture mechanics techniques are all based on Griffith's original studies of the fracture of brittle materials (Ref. 21). One conclusion of Griffith's work is that the strength of brittle materials depends on the presence of cracks in these materials. The strength, S, was related to the crack length by the following formula (derived for an elliptical through crack of length 2a):

$$S = (2E\gamma/\pi a)^{\frac{1}{2}} \qquad (1)$$

where γ is the fracture surface energy of the material and E is Young's modulus. Griffith showed that the fracture behavior of glass containing macroscopic cracks obeyed the above equation.

The theory developed by Griffith was generalized by Irwin (Ref. 21) who established fracture mechanics as a practical science which could be used to assure the reliability of structural materials. In Irwin's analysis the condition for failure could be expressed in the following general form for plane stress deformation:

$$K_I^2 = 2E\gamma \qquad (2)$$

Where K_I is known as the stress intensity factor for opening mode loading.

The stress intensity factor, K_I, occupies a central position in the science of brittle fracture because it is proportional to the

stress near the crack tip. In fact at any point near the crack tip the stress, σ_{ij}, is related to the stress intensity factor by the following equation (Ref. 22):

$$\sigma_{ij} = (K_I/\sqrt{r})\ f_{ij}\ (\theta) \qquad (3)$$

where r is the distance from the crack tip and f_{ij} (θ) is a function of the angle θ from the fracture plane. Eqn. (3) applies to the region near the crack tip for any crack shape, provided the crack is subjected to opening mode loading (all loads are perpendicular to the crack plane). For any particular crack K_I can be related to the applied load by a stress analysis of the crack geometry. Therefore, the applied load can be related to the stresses near the crack tip. For this reason, K_I is the main mechanical parameter that controls the fracture of brittle materials.

The relation between K_I and the applied load has been determined for many different crack configurations (Ref. 23, 24). For a Griffith crack $K_I = S\sqrt{\pi a}$, which is obtained by comparing Eqn. (1) and (2). While the Griffith configuration could be used to obtain fracture information, other crack configurations are easier to use. Two crack configurations that have been used most frequently to obtain fracture mechanics data on glass are the double cantilever beam configuration (Ref. 24, 25) and the double torsion configuration (Ref. 26). Either of these techniques can be used conveniently to obtain fracture mechanics data on glass (Ref. 27, 28).

FRACTURE MECHANICS DATA ON GLASS

Crack Growth Data

The earliest fracture mechanics studies, conducted in nitrogen gas containing various amounts of water vapor (Ref. 29), showed that glass fracture was no simple process. Fracture appeared to occur by several mechanisms as indicated by the tri-modal curves shown in Fig. 2. Three characteristic regions of crack growth were observed. At low values of K_I, region I, the crack velocity, v, depended exponentially on K_I, and also on the parital pressure of water in the environment.

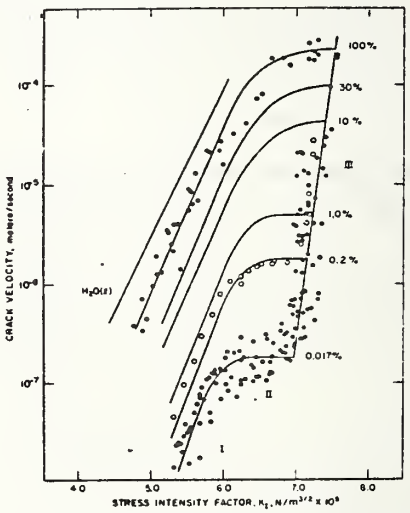

Fig. 2 Effect of water vapor (% R.H.) on crack propagation (Ref. 29)

At higher values of K_I, region II, the crack velocity depended on the partial pressure of water in the environment, but was nearly independent of K_I. Finally at the highest values of K_I, region III, crack growth again depended exponentially on K_I, but now did not depend on water in the environment. In region I and II crack growth was attributed to a chemical reaction between water in the environment and the stressed glass at the crack tip. In region I crack motion was reaction rate limited while in region II crack motion was transport rate limited depending on concentration differences between the crack tip and the bulk environment. In region III crack motion was independent of environment and fracture was due to some process that depends only on the glass structure. More recent studies of fracture in vacuum (see below) indicate that region III does not occur for all glasses.

Crack propagation in region I has been shown to depend on temperature, glass composition and environment. For constant K_I, the crack velocity in water increases as the temperature is increased suggesting that crack growth is an activated process (Ref. 30). A least squares fit of crack growth data for a number of glasses to an Arhenius type equation yields a zero-stress activation energy that ranges from 20 to 30 Kcal/ mol. This range of activation energies is consistent with that expected from a chemical reaction, and is, therefore, consistent with the mechanism proposed by Charles and Hillig for the static fatigue of glass (Ref. 31, 32). In other aqueous environments (acids, bases and various salt solutions) crack propagation has been shown to depend on the pH of the test solution (Ref. 33), Fig. 3.

For example, in silica glass crack propagation curves obtained in high pH solutions have about twice the slope of those obtained in low pH solutions. This change of slope with pH can be used to explain similar slope changes observed for other glasses that were tested in water (Ref. 30). In general, high alkali containing glasses have slopes that are more shallow than the low alkali containing glasses. This difference in slope has been attributed to a difference in pH at the crack tip, the pH being determined by a

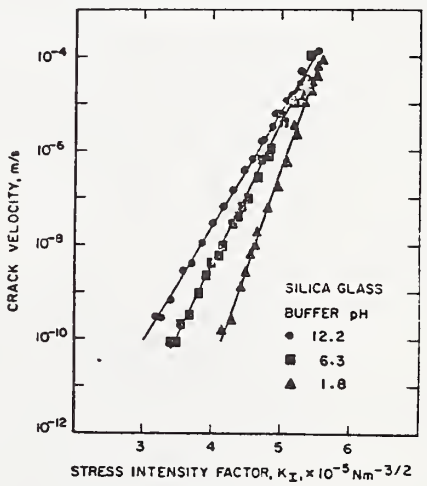

Fig. 3 Effect of pH on crack propagation (Ref. 33)

chemical reaction between the glass and the crack tip solution. The high alkali containing glasses react to form a basic crack tip environment while glasses containing little or no basic constituents react to form an acidic environment.

Region I crack growth has also been investigated in normal alcohols by Freiman (Ref. 34) and by Evans and Wiederhorn (Ref. 35). Tri-modal curves were obtained (Fig. 4) indicating that crack growth behavior in these environments was similar to that in nitrogen gas containing water vapor. At a given value of K_I, the crack velocity was proportional to the concentration of the water in the alcohol, suggesting that crack propagation is mainly due to the water in the alcohol and not to the alcohol itself. However, in region III the alcohol chain length does have a small effect in the position of the crack velocity curve.

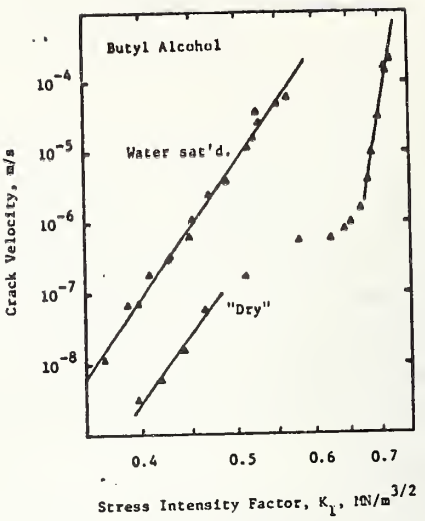

Fig. 4 Crack propagation in Butyl alcohol (Ref. 35)

Information on the mechanism of fracture in region III has been obtained recently by Wiederhorn et al (Ref. 36) from crack propagation studies in vacuum. In these studies, it was observed that the crack growth depended on the composition of the glass. For some glass compositions crack growth in region III depended on temperature in an Arhenian manner (Fig. 5). For other glass compositions slow crack growth did not occur; instead glass fractured abruptly at a critical value of K_I. These differences in behavior apparently depend on the elastic properties of the glass. Crack growth in vacuum occurred for glasses exhibiting normal elastic behavior (the bulk modulus decreasing with increasing temperatures but increasing with increasing pressure). By contrast crack growth did not occur

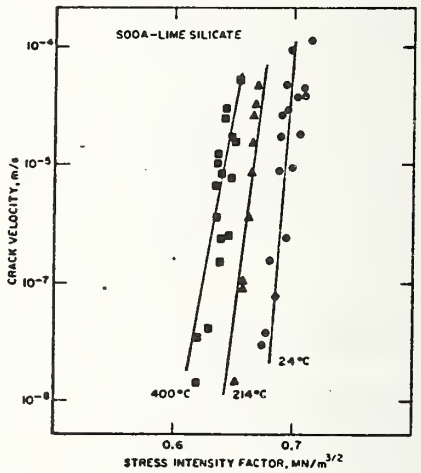

Fig. 5 Crack propagation in vacuum (Ref. 36)

for glasses that exhibited anomolous elastic behavior (the bulk modulus increasing with increasing temperatures, but decreasing with increasing pressure). Wiederhorn et al (Ref. 36) suggested that this difference in behavior could be related to the glass structure near the crack tip. Thomson's theory of "lattice trapping" which relates structure to fracture behavior may explain the fracture behavior of glass in vacuum (Ref. 37, 38). The reader is referred to the original article by Wiederhorn et al (Ref. 36) for a futher discussion of this point.

CRITICAL STRESS INTENSITY FACTOR DATA

In addition to crack propagation studies, fracture mechanics techniques can be used to measure the critical stress intensity factor for abrupt fracture, K_{IC}. Because K_I is related to the stresses and strains near the crack tip, K_{IC} gives a measurement of the maximum stresses or strains that a material can withstand prior to failure. K_{IC} is commonly defined as the value of K_I that is required for crack growth in a inert environment. K_{IC} is a well defined parameter for materials that fail abruptly because of rapid crack acceleration at a well defined value of K_I. However, for materials that exhibit slow crack growth in an inert environment, K_{IC} is not so easily defined because the lower limit of K_I for the initiation of crack motion is not easily measure. For these materials we have defined K_{IC} as the value of K_I (measured experimentally) required for a crack to move at a velocity $\sim 10^{-1}$ m/s. Using this definition, values of K_{IC} have been reported for a number of different glass compositions (Ref: 39, 40). The values of K_{IC} for glass depend on composition and range from 0.6 to 0.9 $MN/m^{3/2}$.

The values of K_{IC} for glass can be used to demonstrate the extreme brittleness of glass. Dugdale (Ref. 41) and McClintock and Irwin (Ref. 42) have shown that a good estimate of the plastic zone size, R, near a crack tip can be obtained from the following equation:

$$R = (\pi/8)\ (K_{IC}/\sigma_y)^2 \qquad (4)$$

where σ_y is the yield stress of the glass. Applying this equation to silica glass (K_{IC} = 0.79 $MN/m^{3/2}$) and soda lime silicate glass (K_{IC} = 0.75 $MN/m^{3/2}$) for which σ_y has been estimated from hardness indentation studies (Ref. 43) to be 19.5 and 10 GN/m^2 respectively, the sizes of the plastic zones at the crack tip calculated from eqn. 4 are 6.4×10^{-10} m for silica glass and 26×10^{-10} m for soda lime silicate glass. The fact that the plastic zone sizes for metals and plastics (1.4×10^{-4} - 14×10^{-4} m for PMMA and 7.1×10^{-4} m

for 4340 steel) (Ref. 44) are so much larger emphasizes the extremely brittle nature of glass. Plastic flow at crack tips in glass does not significantly reduce the stress concentrating effect of surface microcracks.

Comparison of Crack Propagation Data with Strength Data

Crack growth data are of value for engineering purposes only if the data are consistent with strength data obtained at constant load or at constant loading rate. The easiest experimental comparison is between the crack propagation data and the loading rate data.

For most glasses the crack velocity can be expressed as a power function of K_I, $v = AK_I^n$, where A and n are experimentally determined crack propagation parameters. Using this expression, Evans showed that the loading rate, $\dot{\sigma}$, was related to the strength, σ, by the following equation (Ref. 45):

$$\sigma^{n+1} = 2(n + 1)\dot{\sigma}\, \sigma_{IC}^{n-2}/AY^2\, K_{IC}^{n-2}\, (n - 2) \qquad (5)$$

where σ_{IC} is the median strength of the glass measured in an inert environment (vacuum or super dry nitrogen), and Y is the factor that depends on the crack geometry. Using this equation, a comparison between crack propagation data and strain rate data was made for two glasses: a soda lime silicate glass (Ref. 47) and an ultra-low expansion silica glass containing 7.5 percent TiO_2 (Ref. 48). Results for the silica glass tested in water (Fig. 6) show excellent agreement between strength measurement and crack propagation data suggesting that failure was primarily by crack propagation. A similar comparison for soda lime silicate glass tested in nitrogen, one percent R.H., also gives excellent agreement between the crack propagation data and the strength data.

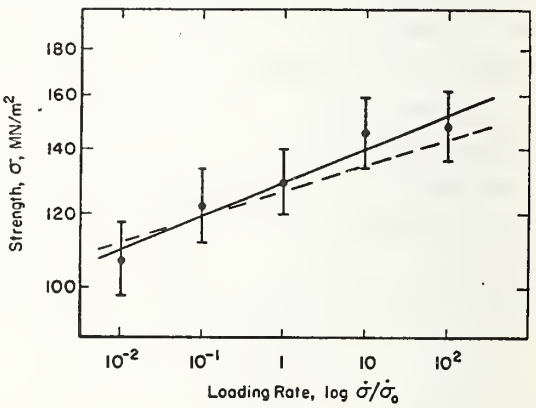

Fig. 6 A comparison of strength and crack propagation data (Ref. 48)

Other less complete comparisons between strength and crack propagation data have been made. In a recent studies on a variety of glasses, Ritter (Ref. 48) reports good agreement for n obtained

from loading rate and crack propagation studies. Slopes determined from constant load studies on silica and soda lime silicate glass in water are also in good agreement with slopes determined from crack propagation studies (Ref. 30).* However, constant load studies on abraded silica glass and on Pyrex glass (abraded and chemically polished) do not agree with crack propagation studies (Ref. 49, 50). This difference in behavior has been attributed to differences in crack tip chemistry for the two types of studies (Ref. 33). Thus, if the pH at the crack tip differed for the two types of studies then differences in slope would be expected. Because the failure time can be estimated from crack growth information, it is of practical importance to resolve these differences in behavior.

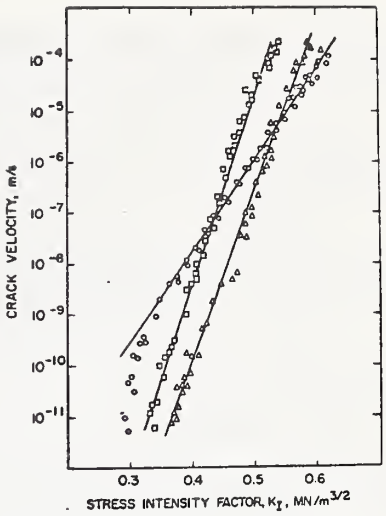

Fig. 7 Crack propagation air (50% R.H.): Δ silica glass; □ pytex; o soda-lime (Ref. 51)

The Static Fatigue Limit in Glass

Fracture mechanics techniques can be used to investigate the static fatigue limit in glass. This limit, which for a given component is the load below which fracture will not occur regardless of how long the component is subjected to load, has been estimated by various authors as 20 to 30 percent of the short term strength (presumably σ_{IC}) (Ref. 10, 19). Fracture mechanics data can also be used to estimate the value of the static fatigue limit in glass. The fatigue limit is determined by the value of K_I at which crack motion stops. Recent studies by Wiederhorn and Johnson (Ref. 51) at crack velocities as low as 10^{-11}m/s gave no indication of a static fatigue limit for Pyrex or silica glass tested in air (50 percent R.H.). The crack velocity data for these glasses approximate a straight line on a logarithmic plot over the entire range of parameters (Fig. 7). The lowest

*In these studies the crack velocity was expressed as an exponential function of K_I, $v = v_o \exp \beta K_I$, and the strength as $\sigma/\sigma_{IC} = 0.5 - (1/\beta K_{IC}) \ln (t/t_{0.5})$, where $t_{0.5}$ is the time to failure at a load $\sigma_{IC}/2$. Termed the universal fatigue curve, this type of strength plot was suggested first by Mould (Ref. 18). For glass, K_I - v data are represented equally well by an exponential or power function of K_I.

values of K_I measured for these glasses suggest that the fatigue limit is less than ∿44 percent of the short term strength for both Pyrex and silica glass. By contrast, the curve for soda lime silicate glass does exhibit severe bending at low velocities suggesting a fatigue limit $K_I \sim 0.3$ $MN/m^{3/2}$, which is ∿40 percent of the short term strength. (Defined here as K_I/K_{IC}). This value is slightly higher than those reported in the literature. If Pyrex is tested in an acid environment (pH < 1.7) one observes a fatigue limit of $K_I \sim 0.41$ $MN/m^{3/2}$ which is ∿53 percent of the short term strength (Ref. 34). This limit results from an aggressive attack of the acid on the glass which causes crack tip rounding.

FRACTURE MECHANICS FOR FAILURE PREDICTION

The excellent agreement between crack propagation data and strength data (Ref. 46, 47) supports the argument that failure in these glasses is by crack growth, and suggests that crack growth data can be used for failure prediction purposes. This use of crack growth data depends on a complete characterization of crack growth for a given application. Once the crack growth has been characterized then the time-to-failure can be calculated provided the size of the critical flaw can be determined. The key to this application of fracture mechanics is in fact the determination of the initial flaw size. Recent work by Evans and Wiederhorn (Ref. 52, 53) suggest that for practical purposes the initial flaw size can be estimated by overload proof testing.

Proof testing is used in structural design to break weak components before they can be placed into service. By so doing we assure the structural integrity of components that are placed in service. In a proof test, a proof test load, σ_p, which is larger than the service load, σ_a, is applied to the components in an inert environment. This procedure guarantees that components passing the proof test have flaws smaller than the critical size that would have resulted in failure during service. In fracture mechanics terms, the stress intensity factor at the crack tip of the most serious flaw, K_p, has to be less than K_{IC} if the component is not to break during the proof test. Thus, for a component to pass the proof test,

$$K_{IC} > K_p = \sigma_p Y \sqrt{a_i} \qquad (6)$$

where Y is a geometric factor and a_i is the crack length of the most serious flaw in the component.

When a component has passed the proof test and is placed into service the stress intensity factor at the most serious flaw is given by:

$$K_i = \sigma_a Y\sqrt{a_i} \tag{7}$$

where σ_a is the service load.

By dividing Eqn. (6) into Egn. (7), the following equation is obtained for the stress intensity factor at the beginning of service:

$$K_i < K_{IC}\ \sigma_a/\sigma_p \tag{8}$$

Thus by proof testing a component prior to service, an estimate of the maximum stress intensity factor at the beginning of service may be obtained.

In service, the component will be gradually weakened by crack growth until failure occurs. The time to failure can be estimated from the definition of crack velocity, $v = da/dt$, and the relation between K_I, a, and σ: ($K_I = \sigma Y\sqrt{a}$). For a constant load

$$v = (2K_I/Y^2\sigma_a{}^2)\ dK_I/dt \tag{9}$$

This equation can be solved to give the following expression for the failure time:

$$t = (2/Y^2\sigma_a{}^2) \int_{K_i}^{K_{IC}} (K_I/v)\ dK_I \tag{10}$$

This equation can be evaluated either numerically or analytically if a relationship between K_I and v is available. For $v = AK_I^n$, a minimum time-to-failure, t_{min}, is obtained by substituting K_i from equation 8 into the lower integration limits of Eqn. (10).

$$t_{min} = 2\sigma_a^{-2}\ (K_{IC}\ \sigma_a/\sigma_p)^{2-n}/AY^2(n-2) \tag{11}$$

Note that all the variables in the right hand side of this equation can be determined experimentally.

The main features of Eqn. (11) is that the minimum time to failure t_{min}, after a proof test is inversely proportional to the service stress squared and directly proportional to a function of the proof test ratio, σ_p/σ_a. In functional form the equation may be expressed as follows:

$$t_{min} = \sigma_a^{-2}\ .\ f(\sigma_p/\sigma_a) \tag{12}$$

The function of proportionality, $f(\sigma_p/\sigma_a)$, is determined from measurements of K_{IC} and from crack growth data. Thus, all the necessary information for failure prediction can be obtained by fracture mechanics techniques.

The relationship given by Eqn. (12) can be presented graphically in the form of a proof test diagram that can be used for design purposes. A diagram of this type is given in Fig. 8 for a low expansion silica glass containing 7.5 percent TiO_2. The diagram gives a plot of the minimum time to failure versus the service stress. Each of the lines on this diagram represents the relationship between t_{min} and σ_a for a given proof test ratio, σ_p/σ_a. The diagram is used to select an appropriate proof test ratio for a specific application. The silica glass represented by this diagram was considered for use as windows in the Space Shuttle, for which the glass was required to sustain a load of 3 MN/m^2 ($\sim$4,000 psi). Assuming that for safe operation the load would have to be supported for one year, a proof test ratio of approximately 2.6 is obtained from the diagram. Thus reliable performance of the space craft windows would require proof testing to a stress of 12 MN/m^2 ($\sim$10,000 psi).

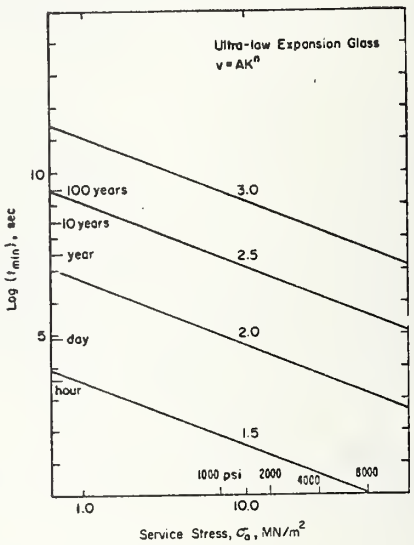

Fig. 8 Proof test diagram (Ref. 47)

The above example of proof testing illustrates the basic procedure that should be followed to assure the reliability of glass for structural application. However, certain precautions are necessary to assure the validity of the method. These precautions are concerned with the accuracy and applicability of the proof test data, the design of a proper proof test procedure and the possibility of strength degradation after the proof test has been completed. These precautions are necessary since an incorrect assessment of any one of them could invalidate the proof test and result in premature component failure. The interested reader is referred to references 52-56 for a more complete discussion of the method and its application to structural design. Despite these precautions, proof testing is a promising method of using fracture mechanics data to assure the reliability of glass structures.

SUMMARY

This paper has summarized the strength and fracture data on glass, emphasizing the phenomenon of static fatigue. In summarizing the strength of glass, it was noted that glass is characterized by extreme brittle behavior. The practical strength is much less than the theoretical strength because of the presence of cracks in the glass surface. The growth of these cracks caused by water in the environment leads to the phenomenon of static fatigue, which is characterized by delayed failure under constant load, or a loading rate dependence of strength.

Static fatigue can be studied by the techniques of fracture mechanics which use specimens that contain large artificially introduced cracks. The key variable that can be measured by fracture mechanics techniques is the stress intensity factor, K_I, which is proportional to the stresses near the crack tip. By relating K_I to the crack velocity, temperature, environment and glass composition it has been demonstrated that the fracture of glass is a complex phenomenon that is controlled by a number of different mechanisms involving chemical reactions, diffusion and glass structure. In cases where a direct comparison has been made between crack growth data and strength data, good agreement is obtained suggesting that crack growth data can be used for design purposes. A method of using fracture mechanics data to obtain proof test diagrams is outlined. These diagrams can be used to select the proof test load that will assure the lifetime of a structural component for a particular application.

ACKNOWLEDGEMENT

The author greatfully acknowledges the support of the office of Naval Research, Contract NAonr 5-73, NR032-535.

REFERENCES

(1) Hillig, W. B., C. R. Symposium sur la résistance mécanique du verre et les moyens de l'améliorer, Union Scientifique Continentale du Verre, Charleroi (1962).
(2) Mallinder, F. P., Proctor, F. P., Phys. Chem. Glasses 5, 91 (1964).
(3) Bridgman, P. W., and Simon, I., J. Appl. Phys. 24, 405 (1953).
(4) Cohen, H. M., and Roy, R., Phys. Chem. Glasses 6, 149 (1965).
(5) Ernsberger, F. M., J. Am. Ceram. Soc. 51, 545 (1968).
(6) Dick, E. and Peter, K., J. Am. Ceram. Soc. 52, 338 (1969).
(7) Ernsberger, F. M., Phys. Chem. Glasses 10, 240 (1969).
(8) Ernsberger, F. M., Prog. Ceram. Sci. 3, 58 (1963).
(9) Grenet, L., Bull. Soc. Encour. Ind. Mat. 4, 839 (1899).
(10) Shand, E. B., J. Am. Ceram. Soc., 37, 52 (1954).
(11) Milligan, L. H., J. Soc. Glass Technol., 13, 341T (1929).

(12) Gurney, C. and Pearson, S., Proc. Phys. Soc., 62, 469 (1949).
(13) Preston, F. W. and Baker, T. C., J. Appl. Phys. 17, 170 (1946).
(14) Preston, F. W. and Baker, T. C., J. Appl. Phys. 17, 179 (1946).
(15) Kropschot, R. H. and Mikesell, R. P., J. Appl. Phys. 28, 610 (1951)
(16) Charles, R. J., Prog. Ceram. Sci. 1, 1 (1961).
(17) Charles, R. J., J. Appl. Phys. 29, 1554 (1958).
(18) Mould, R. E. and Southwick, R. D., J. Am. Ceram. Soc. 42, 489 (1959).
(19) Holland, A. J. and Turner, W. E. S., J. Soc. Glass Technol. 24, 46T (1940).
(20) Griffith, A. A., Phil, Trans. Ray. Soc. (London) 221A, 163 (1920).
(21) Irwin, G. R., Encyclopedia of Physics, Springer, Heidelberg (1958).
(22) Paris, P. C. and Sih, G. C., ASTM Special Technical Publication, No. 381.
(23) Brown, W. F. and Srawley, J. E., ASTM Special Technical Publication No. 410
(24) Srawley, J. E. and Gross, B., Mater, Res. Stand. 7, 155 (1967).
(25) Wiederhorn, S. M., Shorb, A. M. and Moses, R. L., J. Appl. Phys. 39, 1569 (1968).
(26) Evans, A. G., J. Mater. Sci. 7, 1137 (1972).
(27) Evans, A. G., Fracture Mechanics of Ceramics, Plenum Press, New York (1974).
(28) Wiederhorn, S. M., ibid.
(29) Wiederhorn, S. M., J. Am. Ceram. Soc. 59, 407 (1967).
(30) Wiederhorn, S. M. and Bolz, L. H., J. Am. Ceram. Soc. 53, 543 (1970).
(31) Charles, R. J. and Hillig, W. B., C. R. Symposium sur la résistance mécanique du verre et les moyens de l'améliorer, Union Scientifique Continentale du Verre, Charleroi (1962).
(32) Hillig, W. B. and Charles, R. J., High Strength Materials, John Wiley and Sons, New York (1965).
(33) Wiederhorn, S. M and Johnson, H., J. Am. Ceram. Soc. 56, 192 (1973).
(34) Freiman, S. W., J. Am. Ceram. Soc., August (1974).
(35) Evans, A. G. and Wiederhorn, S. M., J. Am. Ceram. Soc., To be published.
(36) Wiederhorn, S. M., Johnson, H., Diness, A. M. and Heuer, A. H., J. Am. Ceram. Soc., July (1974).
(37) Thomson, R., Hsieh, C. and Rana, R., J. Appl. Phys. 42, 3154 (1971).
(38) Hsieh, C. and Thomson, R., J. Appl. Phys. 44, 2051 (1973).
(39) Wiederhorn, S. M., J. Am. Ceram. Soc. 52, 99 (1969).
(40) Wiederhorn, S. M. Evans, A. G. and Roberts, D. E., Fracture Mechanics of Ceramics, Plenum Press, New York (1974).

(41) Dugdale, D. S., J. Mech. Phys. Solids 8, 100 (1960).
(42) McClintock, F. A. and Irwin, G. R., ASTM Special Technical Publication, No. 381.
(43) Marsh, D. M., Proc. Ray. Soc. A279, 420 (1964).
(44) McClintock, F. A. and Argon, A. S., Mechanical Behavior of Materials, Addison-Wesley Publication Co., Inc., Reading, Mass. (1966).
(45) Evans, A. G., Int. J. Fract. Mech., To be published.
(46) Evans, A. G. and Johnson, H., J. Mat. Sci,. To be published.
(47) Wiederhorn, S. M., Evans, A. G., Fuller, E. R., and Johnson, H., J. Am. Ceram. Soc., August (1974).
(48) Ritter, J. E. and Sherburne, C. L., J. Am. Ceram. Soc., 54, 601 (1971).
(49) Ritter, J. E. and Manthuruthil, J., Glass Tech. 14, 60 (1973).
(50) Doremus, R. H., Corrosion Fatigue: Chemistry Mechanics and Microstructure, Nat. Ass. Corrosion Engr. (1972).
(51) Wiederhorn, S. M and Johnson, H., unpublished data.
(52) Evans, A. G. and Wiederhorn, S. M., Int. J. Fract. Mech. (1974), NBS Report No. NBSIR 73-147.
(53) Wiederhorn, S. M., J. Am. Ceram. Soc. 56, 27 (1973).
(54) Evans, A. G. and Fuller, E. R., Met. Trans. 5, 27 (1974).
(55) Evans, A. G. and Fuller, E. R., J. Mech. Phys. Solids, To be published.
(56) Wiederhorn, S. M., To be published in Proceedings of Ceramics for High Performance Application, Hyannis, Nov. 13-16 (1973).

DISTRIBUTION LIST

Organization

Office of Naval Research
Department of the Navy
Attn: Code 471
Arlington, Virginia 22217

Director
Office of Naval Research
Branch Office
495 Summer Street
Boston, Massachusetts 02210

Commanding Officer
Office of Naval Research
New York Area Office
207 West 24th Street
New York, New York 10011

Director
Office of Naval Research
Branch Office
219 South Dearborn Street
Chicago, Illinois 60604

Director
Office of Naval Research
Branch Office
1030 East Green Street
Pasadena, California 91101

Commanding Officer
Office of Naval Research
San Francisco Area Office
50 Fell Street
San Francisco, California 94102

Commanding Officer
Naval Weapons Laboratory
Attn: Research Division
Dahlgren, Virginia 22448

Organization

Director
Naval Research Laboratory
Attn: Technical Information Officer
Code 2000
Washington, D. C. 20390

Director
Naval Research Laboratory
Attn: Technical Information Officer
Code 2020
Washington, D. C. 20390

Director
Naval Research Laboratory
Attn: Technical Information Officer
Code 6000
Washington, D. C. 20390

Director
Naval Research Laboratory
Attn: Technical Information Officer
Code 6100
Washington, D. C. 20390

Director
Naval Research Laboratory
Attn: Technical Information Officer
Code 6300
Washington, D. C. 20390

Director
Naval Research Laboratory
Attn: Technical Information Officer
Code 6400
Washington, D. C. 20390

Director
Naval Research Laboratory
Attn: Library
Code 2029 (ONRL)
Washington, D. C. 20390

Commander
Naval Air Systems Command
Department of the Navy
Attn: Code AIR 320A
Washington, D. C. 20360

Commander
Naval Air Systems Command
Department of the Navy
Attn: Code AIR 5203
Washington, D. C. 20360

Commander
Naval Ordnance Systems Command
Department of the Navy
Attn: Code ORD 033
Washington, D. C. 20360

Commanding Officer
Naval Air Development Center
Aeronautical Materials Div.
Johnsville
Attn: Code MAM
Warminster, Pa. 18974

Commanding Officer
Naval Ordnance Laboratory
Attn: Code 210
White Oak
Silver Spring, Maryland 20910

Commander
Naval Ship Systems Command
Department of the Navy
Attn: Code 0342
Washington, D. C. 20360

Commanding Officer
Naval Civil Engineering Laboratory
Attn: Code L70
Port Hueneme, California 93041

Commander
Naval Ship Engineering Center
Department of the Navy
Attn: Code 6101
Washington, D. C. 20360

Naval Ships R¢D Laboratory
Annapolis Division
Attn: Code A800
Annapolis, Maryland 21402

Commanding Officer
Naval Ships R¢D Center
Attn: Code 747
Washington, D. C. 20007

U. S. Naval Postgraduate School
Attn: Department of Chemistry
and Material Science
Monterey, California 93940

Commander
Naval Weapons Center
Attn: Code 5560
China Lake, California 93555

Commander
Naval Underseas Warfare Center
Pasadena, California 92152

Scientific Advisor
Commandant of the Marine Corps
Attn: Code AX
Washington, D. C. 20380

Commanding Officer
Army Research Office, Durham
Box CM, Duke Station
Attn: Metallurgy ¢ Ceramics Div.
Durham, North Carolina 27706

Office of Scientific Research
Department of the Air Force
Attn: Solid State Div. (SRPS)
Washington, D. C. 20333

Defense Documentation Center
Cameron Station
Alexandria, Virginia 22314

National Bureau of Standards
Attn: Metallurgy Division
Washington, D. C. 20234

National Bureau of Standards
Attn: Inorganic Materials Div.
Washington, D. C. 20234

Atomic Energy Commission
Attn: Metals & Materials Branch
Washington, D. C. 20545

Argonne National Laboratory
Metallurgy Division
P. O. Box 299
Lemont, Illinois 60439

Brookhaven National Laboratory
Technical Information Division
Attn: Research Library
Upton, Long Island, New York 11973

Library
Bldg. 50, Room 134
Lawrence Radiation Laboratory
Berkeley, California 94720

Los Alamos Scientific Laboratory
P. O. Box 1663
Attn: Report Librarian
Los Alamos, New Mexico 87544

Commanding Officer
Army Materials and Mechanics
Research Center
Attn: Res. Programs Office (AMXMR-P)
Watertown, Massachusetts 02172

Director
Metals & Ceramics Division
Oak Ridge National Laboratory
P. O. Box X
Oak Ridge, Tennessee 37830

Commanding Officer
Naval Underwater Systems Center
Newport, Rhode Island 02844

Aerospace Research Laboratories
Wright-Patterson AFB
Building 450
Dayton, Ohio 45433

Defense Metals Information Center
Battelle Memorial Institute
505 King Avenue
Columbus, Ohio 43201

Army Electronics Command
Evans Signal Laboratory
Solid State Devices Branch
c/o Senior Navy Liaison Officer
Fort Monmouth, New Jersey 07703

Commanding General
Department of the Army
Frankford Arsenal
Attn: ORDBA-1320, 64-4
Philadelphia, Pennsylvania 19137

Executive Director
Materials Advisory Board
National Academy of Sciences
2101 Constitution Avenue, N. W.
Washington, D. C. 20418

NASA Headquarters
Attn: Code RRM
Washington, D. C. 20546

Air Force Materials Lab
Wright-Patterson AFB
Attn: MAMC
Dayton, Ohio 45433

Air Force Materials Lab
Wright-Patterson AFB
Attn: MAAM
Dayton, Ohio 45433

Deep Submergence Systems Project
Attn: DSSP-00111
Washington, D. C. 20360

Advanced Research Projects Agency
Attn: Director, Materials Sciences
Washington, D. C. 20301

Army Research Office
Attn: Dr. T. E. Sullivan
3045 Columbia Pike
Arlington, Virginia 22204

Department of the Interior
Bureau of Mines
Attn: Science & Engineering Advisor
Washington, D. C. 20240

Defense Ceramics Information Center
Battelle Memorial Institute
505 King Avenue
Columbus, Ohio 43201

National Aeronautics & Space Adm.
Lewis Research Center
Attn: Librarian
21000 Brookpark Rd.
Cleveland, Ohio 44135

Naval Missile Center
Materials Consultant
Code 3312-1
Point Mugu, California 93041

Commanding Officer
Naval Weapons Center Corona Labs.
Corona, California 91720

Commander
Naval Air Test Center
Weapons Systems Test Div. (Code 01A)
Patuxent River, Maryland 20670

Director
Ordnance Research Laboratory
P. O. Box 30
State College, Pennsylvania 16801

Director
Applied Physics Laboratory
Johns Hopkins University
8621 Georgia Avenue
Silver Spring, Maryland 20901

Director
Applied Physics Laboratory
1013 Northeast Fortieth St.
Seattle, Washington 98105

Materials Sciences Group
Code S130.1
271 Catalina Boulevard
Navy Electronics Laboratory
San Diego, California 92152

Dr. Waldo K. Lyon
Director, Arctic Submarine Laboratory
Code 90, Building 371
Naval Undersea R&D Center
San Diego, California 92132

Dr. R. Nathan Katz
Ceramics Division
U.S. Army Materials & Mechanics
Research Center
Watertown, Mass. 02172

SUPPLEMENTARY DISTRIBUTION LIST

Professor R. Roy
Materials Research Laboratory
Pennsylvania State University
University Park, Pennsylvania 16802

Professor D. H. Whitmore
Department of Metallurgy
Northwestern University
Evanston, Illinois 60201

Professor J. A. Pask
Department of Mineral Technology
University of California
Berkeley, California 94720

Professor D. Turnbull
Div. of Engineering and Applied Science
Harvard University
Pierce Hall
Cambridge, Massachusetts 02100

Dr. T. Vasilos
AVCO Corporation
Research and Advanced Development Div.
201 Lowell Street
Wilmington, Massachusetts 01887

Dr. H. A. Perry
Naval Ordnance Laboratory
Code 230
Silver Spring, Maryland 20910

Dr. Paul Smith
Crystals Branch, Code 6430
Naval Research Laboratory
Washington, D. C. 20390

Dr. A. R. C. Westwood
RIAS Division
Martin-Marietta Corporation
1450 South Rolling Road
Baltimore, Maryland 21227

Dr. W. Haller
Chief, Inorganic Glass Section
National Bureau of Standards
Washington, D.C. 20234

Dr. R. H. Doremus
General Electric Corporation
Metallurgy and Ceramics Lab.
Schenectady, New York 12301

Professor G. R. Miller
Department of Ceramic Engineering
University of Utah
Salt Lake City, Utah 84112

Dr. Philip L. Farnsworth
Materials Department
Battelle Northwest
P. O. Box 999
Richland, Washington 99352

Mr. G. H. Heartling
Ceramic Division
Sandia Corporation
Albuquerque, New Mexico 87101

Mr. I. Berman
Army Materials and Mechanics
Research Center
Watertown, Massachusetts 02171

Dr. F. F. Lange
Westinghouse Electric Corporation
Research Laboratories
Pittsburgh, Pennsylvania 15235

Professor H. A. McKinstry
Pennsylvania State University
Materials Research Laboratory
University Park, Pa. 16802

Professor T. A. Litovitz
Physics Department
Catholic University of America
Washington, D. C. 20017

Dr. R. J. Stokes
Honeywell Corporate Research Center
10701 Lyndale Avenue South
Bloomington, Minnesota 55420

Dr. Harold Liebowitz
Dean of Engineering
George Washington University
Washington, D. C. 20006

Dr. H. Kirchner
Ceramic Finishing Company
P. O. Box 498
State College, Pennsylvania 16801

Professor A. H. Heuer
Case Western Reserve University
University Circle
Cleveland, Ohio 44106

Dr. D. E. Niesz
Battelle Memorial Institute
505 King Avenue
Columbus, Ohio 43201

Dr. F. A. Kroger
University of Southern California
University Park
Los Angeles, California 90007

Dr. Sheldon M. Wiederhorn
National Bureau of Standards
Inorganic Materials Division
Washington, D.C. 20234

Dr. C. O. Hulse
United Aircraft Research Labs
United Aircraft Corporation
East Hartford, Connecticut 06108

Professor M. H. Manghnani
University of Hawaii
Hawaii Institute of Geophysics
2525 Correa Road
Honolulu, Hawaii 96822

Dr. Stephen Malkin
Department of Mechanical Engineering
University of Texas
Austin, Texas 78712

Prof. H. E. Wilhelm
Department of Mechanical Engineering
Colorado State University
Fort Collins, Colorado 80521

Stanford University
Dept. of Materials Sciences
Stanford, California 94305

Dr. R. K. MacCrone
Department of Materials Engineering
Rensselaer Polytechnic Institute
Troy, New York 12181

Dr. D. C. Mattis
Belfer Graduate School of Science
Yeshiva University
New York, New York 10033

Professor R. B. Williamson
College of Engineering
University of California
Berkeley, California 94720

Professor R. W. Gould
Department of Metallurgical
and Materials Engineering
College of Engineering
University of Florida
Gainesville, Florida 32601

Professor V. S. Stubican
Department of Materials Science
Ceramic Science Section
Pennsylvania State University
University Park, Pennsylvania 16802

Dr. R. C. Anderson
General Electric R and D Center
P. O. Box 8
Schenectady, New York 12301

Dr. Bert Zauderer
MHD Program, Advanced Studies
Room L-9513 - VFSC
General Electric Company
P. O. Box 8555
Philadelphia, Penna. 19101

Prof. C. F. Fisher, Jr.
Department of Mechanical and Aero-
space Engineering
University of Tennessee
Knoxville, Tennessee 37916

NBS-114A (REV. 7-73)

U.S. DEPT. OF COMM. BIBLIOGRAPHIC DATA SHEET	1. PUBLICATION OR REPORT NO. NBSIR 74-485	2. Gov't Accession No.	3. Recipient's Accession No.

4. TITLE AND SUBTITLE

Strength of Glass--A Fracture Mechanics Approach

5. Publication Date

6. Performing Organization Code

7. AUTHOR(S)

S. M. Wiederhorn

8. Performing Organ. Report No. NBSIR 74-485

9. PERFORMING ORGANIZATION NAME AND ADDRESS

NATIONAL BUREAU OF STANDARDS
DEPARTMENT OF COMMERCE
WASHINGTON, D.C. 20234

10. Project/Task/Work Unit No. 3130453

11. Contract/Grant No. NR-032-517

12. Sponsoring Organization Name and Complete Address (Street, City, State, ZIP)

Department of the Navy
Office of Naval Research
Code 471, 800 N. Quincy Street
Arlington, Virginia 22217

13. Type of Report & Period Covered Interim
7-1-73 thru 6-30-74

14. Sponsoring Agency Code

15. SUPPLEMENTARY NOTES

16. ABSTRACT *(A 200-word or less factual summary of most significant information. If document includes a significant bibliography or literature survey, mention it here.)*

After a brief review of those factors that determine the strength of glass (brittleness, surface flaws, susceptibility to stress corrosion cracking), a discussion will be given of how fracture mechanics techniques can be used to understand the physics and chemistry of glass strength. In this paper we assume that the strength of glass is limited by the growth of cracks that are always present in normal glass surfaces. Fracture mechanics techniques can be used to characterize the crack growth and to relate the growth to experimental parameters such as temperature, environment and glass composition. Crack growth data obtained in this manner can be used to develop a deeper understanding of fracture mechanisms, and to develop charts that can be used for the design of glass structural components. Examples of both applications are given in the paper.

17. KEY WORDS *(six to twelve entries; alphabetical order; capitalize only the first letter of the first key word unless a proper name; separated by semicolons)*

Crack growth; fracture; glass; static fatigue; strength.

18. AVAILABILITY

[X] Unlimited

[ ] For Official Distribution. Do Not Release to NTIS

[ ] Order From Sup. of Doc., U.S. Government Printing Office Washington, D.C. 20402, SD Cat. No. C13

[ ] Order From National Technical Information Service (NTIS) Springfield, Virginia 22151

19. SECURITY CLASS (THIS REPORT) UNCLASSIFIED

21. NO. OF PAGES 22

20. SECURITY CLASS (THIS PAGE) UNCLASSIFIED

22. Price